X-ray investigations on some liquid crystalline methacrylic polymers with ω-hexyloxysalicylaldimine side groups carrying *p*-alkyl or *p*-alkyloxy terminal substituents

R. WERNER, E. A. SOTO BUSTAMANTE†*, P. A. NAVARRETE ENCINA†, and W. HAASE

Technische Universität Darmstadt, Institut für Physikalische Chemie, Petersenstr. 20, 64287 Darmstadt, Germany
†Universidad de Chile, Facultad de Ciencias Químicas y Farmacéuticas, Olivos 1007, Casilla 233, Santiago 1, Chile

X-ray diffraction data for four different liquid crystalline side group methacrylic polymers based on the ω-hexyloxysalicylaldimine moiety with *p*-alkyl or *p*-alkyloxy terminal substituents are presented. For the decyloxy, dodecyloxy and octyl derivatives, a smectic C_2 phase occurs over a broad temperature range, while for the tetradecyl derivative a complex behaviour was observed on cooling from the isotropic state. In this last case a smectic A_d phase arises, changing to a smectic C_2 phase and a further smectic C_d phase. A possible explanation for the observed phenomena is presented.

1. Introduction

Side group liquid crystalline polymers continue to be the focus of considerable research activity, not only because of their application potential in advanced electro-optic devices [1], but also because they provide quite demanding challenges to our understanding of self-assembly in condensed matter [2].

The aim of this research was to clarify the unusual properties of liquid crystalline mixtures of achiral side group polymers with their respective monomer. One interesting goal is to increase the observed values of the macroscopic polarization in such mixtures in comparison with that for similar compounds already described in previous reports [3]. For designing new materials with targeted properties, the relationship between the structure and properties of materials must be understood. To achieve this, it is necessary to identify the mesophases observed in pure samples of polymers and monomers and to correlate the observed properties with the length of the terminal chain and with other aspects of chemical structure.

To understand the observed unusual antiferroelectric phenomenon in mixtures of side group liquid crystalline polymers and their related monomer, four new liquid crystalline side group polymers with different terminal chains were synthesized, characterized and compared with our previously investigated samples [4]. The acronym used is (P)M6R*m* in accordance with our previous work, where P denotes the polymer backbone. M6R indicates the presence of a methacrylate group with six methylene units acting as a spacer (M6) and bonded to the rigid core (R). The core consists of a resorcylphenylimine group. The phenylimine group possess in its *para*-position either a terminal alkoxy (*m*) or alkyl tail (*m*n) with *m* methylene units (see figure 1).

*Author for correspondence; e-mail: esoto@ciq.uchile.d

2. Experimental

The synthesis of (P)M6R8n and (P)M6R14n has been reported in a previous communication [5]. The preparation of the alkyloxy compounds (P)M6R10 and (P)M6R12 was carried out using a convergent synthetic pathway already described [6, 7]. The compounds investigated were characterized by ^{1}H NMR spectroscopy using a 300 MHz spectrometer (Bruker, WM 300), infrared spectroscopy (FTIR Paragon spectrometer, 100PC) and elemental analysis (Perkin Elmer, 240 B). As examples, the analytical data for only M6R10 and the related polymer PM6R10 are presented.

M6R10. ^{1}H NMR, δ ppm, $CDCl_3$: 13.96 (s, 1H, Ph−O*H*); 8.50 (s, 1H, Ph−C*H*=N); 7.22 (m, 3H, Ph−*H*); 6.92 (m, 2H, Ph−*H*); 6.46 (m, 2H, Ph−*H*); 6.10 (m, 1H, *trans* *H*−C=C−CH_3); 5.55 (m, 1H, *cis* *H*−C=C−CH_3); 4.16 (t, 2H, CH_2−O_2C); 3.98 (m, 4H, CH_2−OPh); 1.94 (s, 3H, CH_3−C=C); 1.83–1.27 (m, 24H, −CH_2−CH_2−CH_2−CH_2−); 0.88 (t, 3H, −CH_2−CH_3). $J_0 = 6.6$ Hz. IR (KBr), cm^{-1}: 1707 s (*v* C=O), 1626 m (*v* C=N), 1299 m, 1250 m, 1199 w,

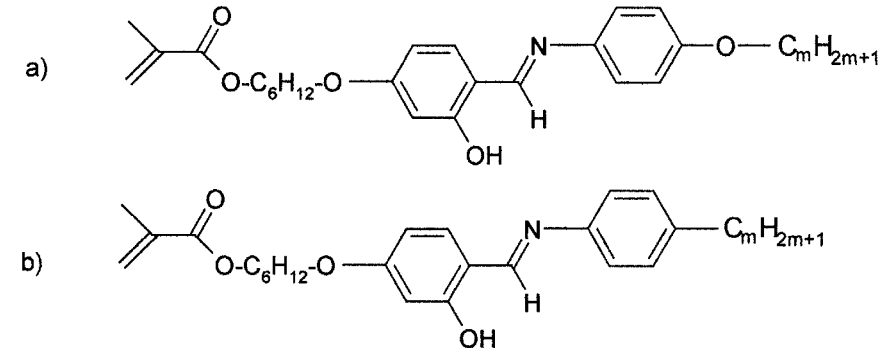

Figure 1. General structures for the monomers investigated: (*a*) M6R10 ($m = 10$), M6R12 ($m = 12$); (*b*) M6R8n ($m = 8$), M6R14n ($m = 14$).

1163 w, 1135 m, (*v* C–O), 642 m, 579 m, 534 m, 504 w, 465 w, 438 w. Elemental analysis: calc. for $C_{33}H_{47}NO_5$, $M = 537.74$, C 73.71, H 8.81, N 2.60; found C 73.18, H 8.77, N 2.56%.

PM6R10. ^{1}H NMR, δ ppm, $CDCl_3$: 13.85 (s, 1H, Ph–O*H*); 8.33 (s, 1H, Ph–C*H*=N); 7.10 (m, 3H, Ph–*H*); 6.80 (m, 2H, Ph–*H*); 6.37 (m, 2H, Ph–*H*); 3.99 (t, 2H, CH_2–O_2C); 3.84 (m, 4H, CH_2–OPh); 1.78–1.25 (m, 27H, –CH_2–CH_2–CH_2–CH_2–; CH_3–C–C_3); 0.87 (t, 3H, –CH_2–CH_3). IR (KBr), cm^{-1}: 1728 s (*v* C=O), 1618 s (*v* C=N), 1296 s, 1251 s, 1190 s, 1168 w, 1139 m, 1117 m (*v* C–O), 684 m, 585 m, 534 s, 465 m. Elemental analysis: calc. for $(C_{33}H_{47}NO_5)_n$, $(M = 537.74)_n$, C 73.71, H 8.81, N 2.60; found C 73.43, H 8.82, N 2.65%.

The molecular mass $\bar{M}_w$, polydispersity index *DI* (calculated from the ratio $\bar{M}_w/\bar{M}_n$) and the degree of polymerization P_w were determined by gel permeation chromatography (GPC) (Waters 510 microflow pump and Waters RI 410 detector) on ultrastyragel columns using tetrahydrofuran as eluent at a rate of 1 ml min^{-1}. The standard polymer used was polystyrene (PS).

The phase transition temperatures were determined using differential scanning calorimetry (Perkin Elmer, DSC-7) with an accuracy of ± 0.1 K.

A polarizing microscope (Leitz, Orthoplan Pol) in conjunction with a hot stage (Mettler, Hotstation FP82) and an SVHS video system (Sony, Panasonic) allowed observation of the phase transitions and the mesomorphic textures for samples mounted between glass plates.

X-ray measurements were carried out using CuK_α-radiation. The samples were contained in 1.0 mm glass capillaries (Lindemann) and held in a copper block. Data for aligned samples in the small angle region were obtained using a focusing horizontal two-circle X-ray diffractometer (STOE, STADI 2) with a linear position sensitive detector [8, 9]. The temperature was stabilized within the range 30 to 250°C at ± 0.5°C during the measurements.

3. Results

The transition temperatures were confirmed by DSC and optical microscopy. The phase sequences of the materials are given in table 1. In the same table the molecular masses $\bar{M}_w$, polydispersion indices *DI* and degrees of polymerization P_w are included. The observed values confirm the polymeric nature of the samples.

Table 2 summarizes the molecular lengths *L* for the side groups calculated using MOPAC93 molecular approximation software, together with other X-ray data for the layers. *L* is the distance along the side group in its extended conformation between the last carbon atom of the aliphatic terminal chain and the first ethylenic carbon atom of the corresponding methacrylate monomer.

Table 1. Phase transition temperatures and enthalpies obtained on heating for the samples investigated, as well as the average molecular mass $\bar{M}_w$, polydispersity index *DI* and degree of polymerization P_w for each of the LC polymers.

Sample	Mesophase	Enthalpy/J g^{-1}	$\bar{M}_w$ (g mol^{-1})	*DI*	P_w
M6R10	Cr–52.0–SmA–97.7–I	83.5–15.6			
M6R12	Cr–46.5–SmA–97.5–I	85.4–15.1			
M6R8n	Cr–44.2–SmA–64.4–I	n.d.[a]			
M6R14n	Cr–55.0–SmC–57.6–SmA–71.6–I	95.4[b]–14.4			
PM6R10	g–n.d.–SmC_2–190.3–I	22.1	104, 300	2.370	194
PM6R12	g–n.d.–SmC_2–190.5–I	21.2	108, 100	2.609	191
PM6R8n	g–n.d.–SmC_2–146.9–I	n.d.		n.d.	
PM6R14n	g–n.d.–SmC_d–148.6–SmC_2–160.7–SmA_d–178.0–I	0.02–1.5–13.6	126, 300	2.570	219

[a] n.d. = not determined.
[b] Enthalpy corresponding to both the SmA and SmC transitions.

Table 2. Calculated lengths of the side groups L, average molecular distances in the layers D, experimental interlayer distances d, calculated ratios $d/2L$ and tilt angles β for the mesophases

Polymer	L/Å	D/Å	d/Å	$d/2L$	β/°	Temp./°C
PM6R10	33.11	4.63	60.09	0.91	24.50	89.7
PM6R12	35.61	4.59	63.67	0.89	27.13	89.7
PM6R8n	29.24	4.73	53.30	0.91	24.50	110.0
PM6R14n	38.20	4.69	62.78	0.82	34.91	149.8

The X-ray diffractograms below the isotropic transition point showed sharp small angle peaks reflecting the smectic character for all the mesophases (see figure 2) and diffuse wide angle halos (see figure 3) related to the degree of disorder within the smectic layers.

The experimental interlayer spacings d, taken from the X-ray measurements, are shown in figures 4 and 5. From these values, the average interlayer distance and the ratio $d/2L$ are calculated. These are included in table 2 and correspond to the given temperatures.

The X-ray data for each one of the investigated polymers will now be discussed.

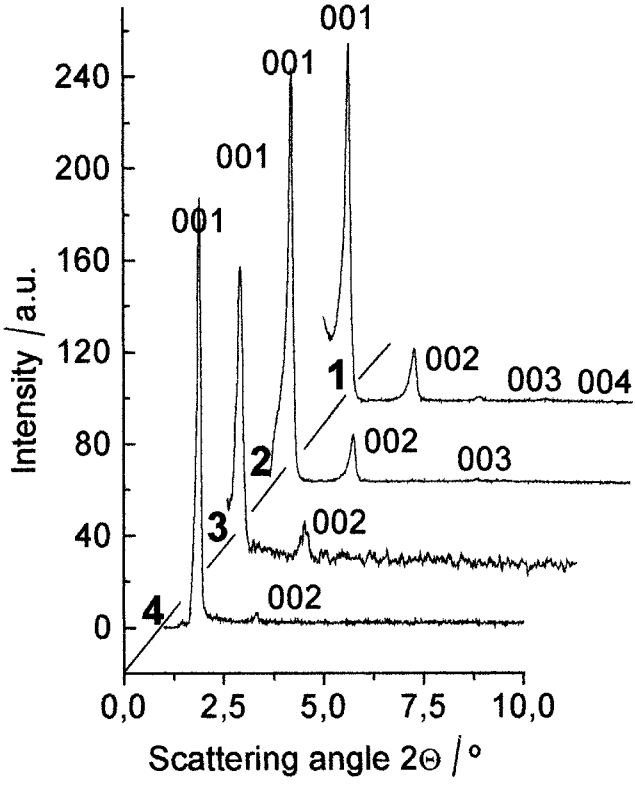

Figure 2. X-ray diffraction patterns in the small angle scattering region for PM6R10 (1) at 120°C; PM6R12 (2) at 120°C; PM6R8n (3) at 140°C and PM6R14n (4) at 176°C in the smectic C_2 phase.

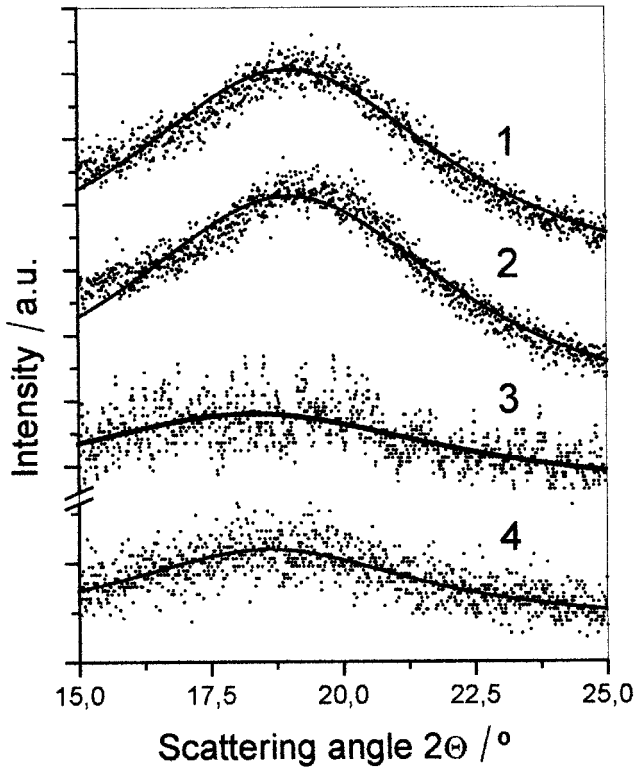

Figure 3. Diffuse wide angle halos, showing liquid-like in-plane order: PM6R10 (1); PM6R12 (2); PM6R8n (3) and PM6R14n (4). The solid lines correspond to the Lorentzian fit of the data.

PM6R10. Trace 1 in figure 2 presents the small angle region at 120°C. Reflections (0 0 1) up to the fourth order (0 0 4), not shown here, could be detected. The position of (0 0 1) is in good agreement with a bilayer structure. The interlayer distances decrease slightly on decreasing the temperature (see figure 4, curve 1). The results, together with those from polarizing optical microscopy, prove the existence of a smectic C phase. The decrease of the d-values on cooling is mainly due to the increase in the tilt angle β within the layer. Taking the interlayer distance and full molecular length (33.11 Å, see table 2), we can calculate the tilt angle β ($\beta = \arccos d/2L$) to be 26.5°–23.1° (see table 2).

PM6R12. The small angle reflections (0 0 1) at 120°C correspond to the first, second and third order (see figure 2, trace 2). Curve 2 in figure 4 displays the temperature dependence of the interlayer distance. The observed d-values are mainly constant over the whole temperature range of the mesophase. The increase in the interlayer distance from 60 Å for PM6R10 to 64 Å in PM6R12 is twice the increase in the length of the terminal chain calculated from the theoretical values using a smaller calculated tilt angle ranging between 27.1° and 26.1° (see table 2).

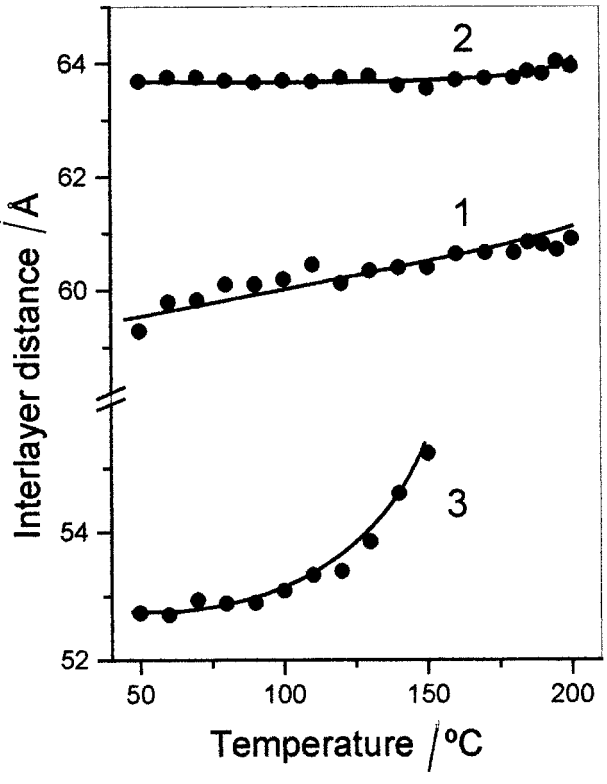

Figure 4. Temperature dependence of the interlayer distance in the smectic C_2 phase for PM6R10 (1); PM6R12 (2) and PM6R8n (3) on cooling.

PM6R8n. The small angle reflections at 140°C (see figure 2, trace 3) show the first and second orders. Figure 4, curve 3, displays the temperature variation of the interlayer distance. Here the *d*-values show an exponential-like increase on heating that gives more evidence for a smectic C phase. The calculated tilt angle β is in the range 25.6°–22.9° (table 2).

PM6R14n. The temperature variation of the first order reflection, a relevant indicative parameter for the interlayer spacing *d*, shows the existence of three different regions in the mesophase (see figure 5). The observed isotropic to smectic A_d and smectic A_d to C_2 transitions for region I correlate reasonably well with the transition temperatures obtained by DSC (see figure 6). The third transition from smectic C_2 to C_d is observed at 148.6°C by DSC and at 132°C by X-ray. This difference in temperature may be explained by a stabilization of the smectic C_2 phase due to surface tension forces in the capillaries. At higher temperatures this phenomenon was not observed, probably due to the low viscosity of the sample in these mesophases.

On cooling from the isotropic state into the mesophase, an increase in the *d*-values from 62.3 Å at 176.3°C, reaching a maximum of 64.5 Å at 159.2°C, was observed (region I). The decrease in the *d*-values on cooling in region II starting from 64.5 Å at 159.2°C and ending with 61.7 Å at 132°C, indicates the existence of a tilted lamellar structure in region II. At 132°C, a third phase transition was observed accompanied by a sudden fall in the *d*-value from 61.7 to 60.7 Å. In region III the *d*-value increases from 60.7 Å at 132°C to 61.1 Å at 109°C. For regions II and III the estimated tilt angle varies between 37.4° and 32.5°.

4. Discussion

In the case of monomers M6R6 and M6R8 reported in previous work [4], the interlayer spacing in the

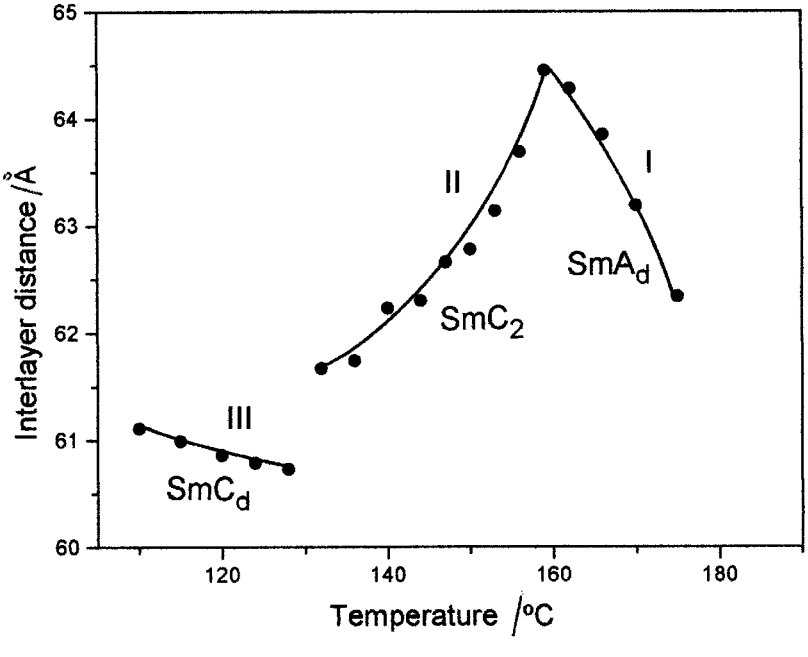

Figure 5. Temperature dependence on cooling of the layer spacing in the smectic phases for PM6R14n.

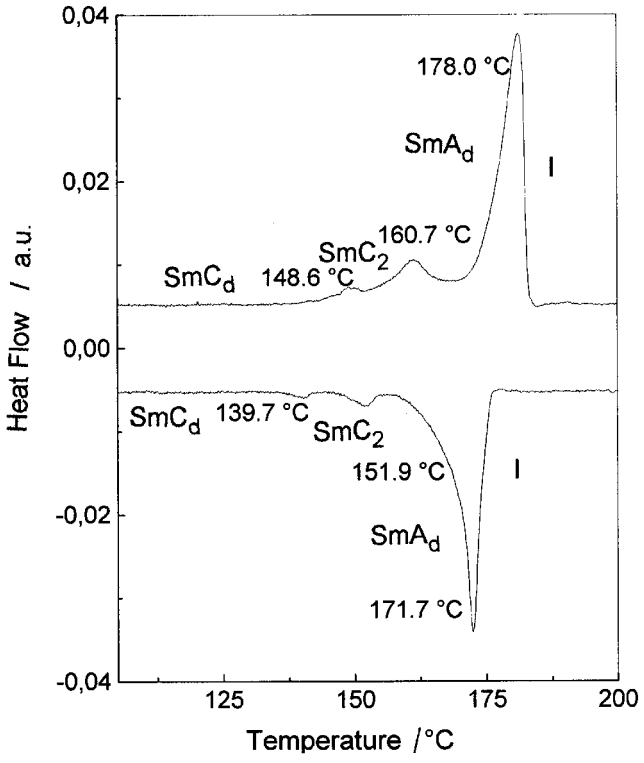

Figure 6. DSC trace for PM6R14n on cooling and on heating at a rate of 10°C min^{-1}.

smectic phase is close to the molecular length, indicating a smectic A layering. The same is true for the monomer M6R8n. For M6R10 and M6R12, the presence of smectic C and A phases was detected by DSC and polarizing optical microscopy. A more detailed study on these monomers will be published as soon as possible.

The situation for M6R14n is different. On heating, a smectic A phase was identified by texture observation. On cooling from the isotropic state, at low cooling rates, this monomer shows a phase transition by DSC at around 57°C, corresponding to the transition from the liquid crystalline to the solid state. This transition occurs over a 2.5°C range, and it is possible to distinguish at least three peaks. Using polarizing optical microscopy, a continuous appearance of perpendicular stripes in the developed fan-shaped texture of the smectic A phase occurs, indicating a change to a smectic C phase close to the solid state transition.

The behaviour for the four related polymers is different. Only the alkyloxy chain compounds show small angle reflections at higher orders (see figure 2). We attribute this behaviour to a smaller ordering between the layers because of the increased flexibility in the molecules of the alkyl chain compounds.

The broad peaks in the wide angle region permit us to calculate the average intermolecular distances D within the smectic layers (see figure 3 and table 2). These peaks were fitted by Lorentzian line shapes (solid lines). Thus molecular packing within the smectic layers must be considered as liquid-like. In the case of the alkyl chain compounds the peaks are wider than for the alkyloxy materials. Therefore the alkyl chains impart a higher disorder to the lateral groups inside the layers thus contributing a lesser degree of compactness in the layers.

For all compounds studied, the interlayer distance is smaller than twice the length of the side groups (table 2, $d/2L$), which is typical for a smectic C_2 phase. Figure 4 shows the temperature dependence of the tilt angle in the smectic C_2 phase for PM6R8n, PM6R10 and PM6R12. As the length of the side group increases from 29.2 Å in PM6R8n to 35.6 Å in PM6R12, the temperature dependence becomes less evident. There is a compensation in the growth of the tilt angle as the temperature decreases. This fact can be attributed to the contribution to the statistical disorder of the longer side group attached to the polymeric backbone.

A more peculiar situation is observed for PM6R14n (see figure 5). The temperature variation of the interlayer spacing d of the first order reflection in the mesophases is rather atypical, indicating the existence of three different structural arrangements, also confirmed by DSC (see figure 6). On cooling from the isotropic state into region I (see figure 5), an interdigitated smectic A phase is indicated. In that region, on decreasing the temperature, the molecular overlapping decreases, accompanied by an increase in the interlayer distance, until reaching a maximum value of 64.5 Å. There is still an overlapping of about 12 to 14 Å when the calculated molecular length L (table 2) and the experimental d-values are considered. A similar behaviour was observed in polysiloxane side group copolymers [10], for which a comparable amount of interdigitation was calculated (7.5 Å).

For region II, beginning below the maximum, packing occurs as in a smectic C_2 phase. The lateral groups start to tilt and because of this, a decrease in the d-values on cooling is observed, again typical for smectic C phases.

Interestingly the transition between regions II and III is associated with a 1.5 Å jump in the interlayer distance and a small change in enthalpy (see figure 5). At this transition, the interdigitation of the tilted side chains in region III became stronger. On further cooling, the d-values in region III increase smoothly, similarly to the d-values in region I. Because of these similarities we assume the existence of a C_d phase in region III analogous to the A_d phase in region I. Of course more detailed X-ray studies are necessary.

A strong item of evidence for the existence of a tilted bilayered smectic C phase in the new polymeric

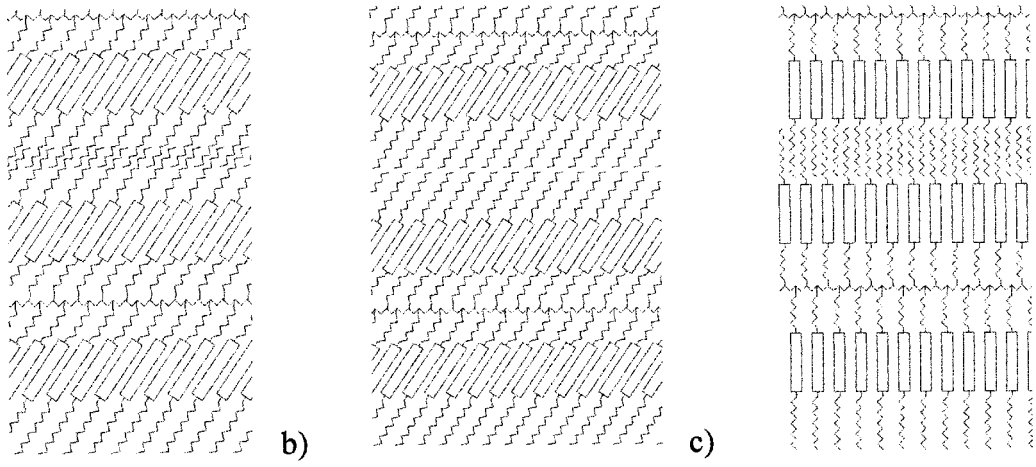

Figure 7. Structural models for the liquid crystalline phases in the polymers: (*a*) interdigitated smectic C_d phase (PM6R14n only); (*b*) smectic C_2 phase; (*c*) interdigitated smectic A_d phase (PM6R14n only).

compounds with aliphatic end chains (PM6R8n and PM6R14n) is the pyroelectric response observed in mixtures of these polymers and their monomers, and already reported in a separate communication [5]. Although these experiments are related to polymer–monomer mixtures, our results on PM6R8 [3] demonstrate close similarities between the mesophases involved in the mixtures and in the pure polymer itself.

5. Conclusions

There is a clear and remarkable difference between the alkyl and alkyloxy polymers. The alkyloxy samples show a relatively smooth change in the interlayer distance on changing the temperature, but the alkyl chain polymer PM6R8n shows a strong and almost non-linear dependence.

The alkyloxy compounds show higher transition temperatures (table 1) as compared with the alkyl compounds and more compactness of side groups, as evidenced by the shape of the diffraction curves in the wide angle region (see figure 3).

Compounds PM6R10, PM6R12 and PM6R8n are ordered in a smectic C_2 phase over the whole temperature range investigated, whereas compound PM6R14n behaves differently. On cooling, a phase sequence smectic A_d, smectic C_2 and smectic C_d could be rationalized. Figure 7 displays structural models for the three observed smectic phases.

In consideration of these results, it is reasonable to expect pyroelectric responses in mixtures of these polymers with their monomers.

E. A. Soto Bustamante is grateful for financial support from Projects FONDECYT 2000 Nr. 1000845 and 7000845. Financial support from Volkswagen Stiftung is also acknowledged.

References

[1] Blinov, L. M., and Chigrinov, V. G., 1996, *Electrooptic Effects in Liquid Crystal Materials* (New York: Springer-Verlag).
[2] Petty, M. C., Bryce, R., and Bloor, D., 1995, *Molecular Electronics* (London: Hodder Headline).
[3] Soto Bustamante, E. A., Yablonskii, S. V., Ostrovskii, B. I., Beresnev, L. A., Blinov, L. M., and Haase, W., 1996, *Liq. Cryst.*, **21,** 829.
[4] Ostrovskii, B. I., Soto Bustamante, E. A., Sulianov, S. N., Galyamedtinov, Yu., and Haase, W., 1996, *Mol. Mater.*, **6,** 171.
[5] Soto Bustamante, E. A., Navarrete-Encina, P., Weyrauch, T., and Werner, R., 2000, *Ferroelectrics*, **243,** 125.
[6] Soto Bustamante, E. A., Galyametdinov, Yu. G., Griesar, K., Schuhmacher, E., and Haase, W., 1998, *Macromol. Chem. Phys.*, **199,** 1337.
[7] Soto Bustamante, E. A., and Haase, W., 1997, *Liq. Cryst.*, **23,** 603.
[8] KläMke, W., Fan, Z. X., Haase, W., Müller, H. J., and Gallardo, H. D., 1989, *Ber. Bunsenges. Phys. Chem.*, **93,** 478.
[9] Fan, Z. X., and Haase, W., 1991, *J. chem. Phys.*, **95,** 6066.
[10] Kozlovsky, M. V., Soto Bustamante, E. A., and Haase, W., 1996, *Liq. Cryst.*, **20,** 35.